International Journal of Engineering Research & Management Technology ISSN: 2348-4039

January- 2015 Volume 2, Issue-1

Email: editor@ijermt.org www.ijermt.org

Weak Links in Mgb_2 Thin Films

Rahul Solanki, Ajay Kumar
SRM University
NCR Campus Ghaziabad

Kavindra Kumar
Baskaracharya College of Applied Science
University of Delhi (New Delhi)

ABSTRACT
Since the discovery of its superconducting properties in 2001, magnesium diboride has generated terrific scientific and engineering research interest around the world. To realize superconducting Josephson devices based on this material that can be implemented further in electronic circuits, crystalline grown MgB_2 thin films are preferred. Presence of weak links in high T_c materials due to its short coherence length and insulating grain boundaries limits the application potential of those materials. These weak links leads to lower critical current density and lower critical field of superconductors and leads to losses. This paper focuses on two types of weak links: ramp- type Josephson junctions and nano bridges formed in MgB_2 thin films. The fabrication and properties of these weak links are discussed over here.

Key Words: Nano Bridge, diboride, Mgb2

1. INTRODUCTION

The exploration of suitable weak link configurations in MgB_2 thin films is an important aspect towards the realization of electronic devices. Less anisotropy, fewer material complexities, strong links between grain boundaries [1] and a longer coherence length ($\xi \sim 5$ nm) compared to high- temperature superconductors (HTS) make MgB_2 feasible to realize good Josephson junctions. Besides the larger critical temperature of MgB_2 as compared to the low- T_C materials, a further positive aspect is the larger charge carrier density of MgB_2 as compared to the high- T_C materials, which is deemed to be beneficial, e. g., for the noise properties of Josephson devices. Furthermore, taking into account the multiband nature of superconductivity, which has as a consequence the existence of two different gaps in MgB_2, large I_CR_N products are feasible, as was recently pointed out by Brinkman et al. [2]. For tunneling in the direction of the a-b plane of MgB_2 an I_CR_N product of 5.9 mV at T = 4.2 K is predicted and 4.0 mV for tunneling in the c- axis direction. Films prepared by PLD were used for the realization of ramp-type Josephson junctions. Our first realizations of such types of MgB_2 Josephson junctions showed a modulation of the critical current of the junctions in a magnetic field and the appearance of Shapiro steps by applying microwave irradiation, as will be described in detail below. Fabrication of nano bridges is an alternative method for the formation of weak links. Nano bridges were formed in epitaxial thin films grown by the HPCVD method. The high quality films had a very high critical current density of about $5x10^7 A/ cm^2$ at 4.2 K [5].

The deposition of MgB_2 films on a polycrystalline Al_2O_3 substrates is obtained by the reaction between evaporated magnesium atoms and boron atoms that decompose from diborane near the heaters [4]. The superconducting MgB_2 films show a transition temperature at 38.5 K and a zero-resistance temperature at 38 K. The critical current density of the films is $10^5 A/cm^2$[7]. By using hybrid physical-chemical vapor deposition (HPCVD) method, MgB_2 thin films were fabricated on silicon substrates with buffers of alumina grown by using atomic layer deposition

method. The growth conditions were in a range of growth temperatures of 500–600 °C and under the reactor pressures of 25–50 Torr [6].

An improved hybrid physical chemical vapor deposition (HPCVD) method for the preparation of magnesium diboride (MgB_2) films is proposed. The superconducting MgB_2 films show a transition temperature at 38.5 K and a zero-resistance temperature at 38 K. The critical current density of the films is 10^5 A/cm^2[12]. By using hybrid physical-chemical vapor deposition (HPCVD) method, MgB_2 thin films were fabricated on silicon substrates with buffers of alumina grown by using atomic layer deposition method. The growth conditions were in a range of growth temperatures of 500–600 °C and under the reactor pressures of 25–50 Torr [11].

The growth of high-quality MgB_2 films by thermally decomposing decaborane ($B_{10}H_{14}$) in Mg vapor. We grew MgB_2 films on c-cut sapphire substrates held at 400–450 °C by supplying vaporized $B_{10}H_{14}$ into a pocket heater with high Mg vapor pressure. The resultant films as thin as 100 nm showed strong and sharp c-axis lattice peaks in X-ray diffraction, indicating nearly ideal epitaxial growth [13].

The growth of MgB_2 films by pyrolysis of decaborane ($B_{10}H_{14}$) in Mg vapor was discussed by yamazaki and Naito [14]. Increasing the growth temperature, this reaction becomes noticeable and leads to the formation of MgO and $Mg_{1-x}Al_xB_2$, which deteriorates the properties of resultant MgB_2 films. Recently, Superconducting MgB_2 thin films with different thicknesses were fabricated by excess Mg using sequential electron beam evaporation technique. The flux rate of Mg and B were chosen as 3 nm/sn and 0.5 nm/sn respectively. The thickness of Mg/B layer was determined as 3/1 which causes an excess Mg for MgB_2 formation [15].

2. RAMP- TYPE JOSEPHSON JUNCTIONS BASED ON PLD THIN FILMS

A Josephson junction consists of two electrodes separated by a barrier layer, which can be an insulator or a normal metal. Ramp-type junctions [3] have been developed for high-T_C superconductors to obtain electrical transport through the barrier of the junction in the direction of the a-b plane of the crystal lattice in thin films grown with the c- axis perpendicular to the substrate surface. Advantages of using this configuration for MgB_2 Josephson junctions are that possible degradation of superconducting properties at the surface of MgB_2 will not be reflected in the junction and that the junction area can be made small. Degradation of the superconducting properties at the surface can occur due to several reasons such as an Mg deficiency in the top part of the film or the presence of an Mg capping layer depending on the thin film growth procedure. Since one of the dimensions of the junction is determined by the film thickness, the width of the junction can be varied to result in small junction areas.

2.2. Electrical Characteristics

The electrical transport properties of the junctions were measured in a four point configuration in a shielded cryostat. The transition temperatures of both electrodes were typically 23 K. This reduced critical temperature as compared to the bulk value is attributed to the small MgB_2 grain size and to impurities of the starting material as well as in the film. Resistively Shunted Junction (RSJ) - like current- voltage characteristics were obtained up to 16 K, albeit with an excess current. Above this temperature, the super current was suppressed by the thermal noise. Fig. 2 (a) displays the I-V characteristic of a 7μ m wide junction at T = 3.6 K, exhibiting an excess current of 30%.

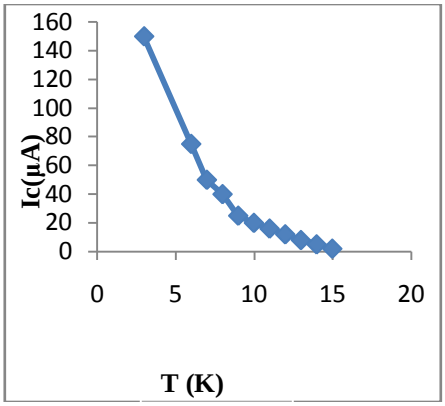

Fig- 2 (a)

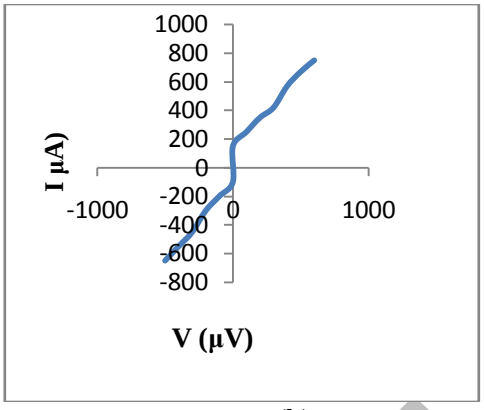

Fig- 2 (b)

Fig. 2 (a) I-V characteristics of a 7 μm wide junction at T = 3.6 K. (b) Critical current vs. temperature dependence.

At 4.2 K the I_C - value is 130μ A (using a voltage criterion of 5μ V) and taking the slope of 20° of the junction in to account for the determination of the junction area, a corresponding critical current density in order of 1kA/ cm^2 was estimated. The normal state resistance R_N is almost temperature- independent and has a value of about 1Ω. The I_CR_N product is thus 130μV at T = 4.2 K. In fig. 2 (b), the dependence of the critical current on temperature is Presented.

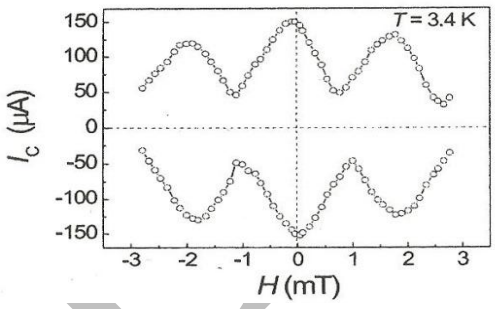

Fig. 3. Modulation of the critical current by a magnetic field applied perpendicular to the current direction and parallel to the substrate, measured at T = 3.4 K.

The application of a magnetic field H perpendicular to the current direction and parallel to the substrate resulted in a modulation of the critical current (Fig. 3). A suppression of the critical current by up to 70% was observed. The I_C (H)-dependence differs from the Fraunhofer dependence that is expected for a small junction with a uniform current distribution, with the large amplitude of the side- peaks and the incomplete suppression of the critical current being signatures of a non- homogeneity of the barrier. This non- homogeneity originates most likely from the roughness of the ramp area after the etching of the ramp, which will show an imprint in the surface roughness of the deposited film.

3. NANOBRIDGES MADE IN HPCVD FILMS

3.1. Nanobridges as weak links

Apart from barrier- layer type Josephson junctions, nanobridges can be utilized as weak links, which can be used to form a SQUID. A number of s on low- T_C superconductor SQUIDs based on nanobridges were published and the first reports of SQUIDs based on nanobridges in high-T_C superconductors appeared in [8]. In Fig. 5 the forces acting on the vortices in a nanobridge are schematically presented. A transport- current that passes through the bridge induces a magnetic field, which can penetrate the superconductor in the form of Abrikosov vortices if the field is larger than the lower critical field H_{C1}. Two of such vortices, with opposite orientation, will then be created simultaneously at the edges of the bridge. An edge- pinning force F_{pin} will act on the vortices. By increasing the transport current the Lorentz force F_L acting on the vortex will overcome this pinning. Consequently, for bias currents exceeding the critical current, the vortices will move towards each other and finally annihilate. During the vortex motion an electric field is induced in the direction of the transport current and energy dissipation will take place.

The Abrikosov vortices have a normal core of the size of the coherence length radius (ξ). Eskildsen et al. [9] measured on MgB_2 single crystals from the vortex core the value of the coherence length in the a-b plane for the p band and found this to be about 50 nm. They estimated from the BCS expression the coherence length in the same plane for the band to be 13 nm, which is well in agreement with the coherence length obtained from H_{C2} measurements. On the other hand, the most common number for ξ used in calculations is about 5 nm, as reported in [10]. The normal core area in the bridge will act as a Josephson weak link for superconducting bridges that are smaller than a few times ξ. In this case a specific relationship exists between the super current and the phase change of the macroscopic wave function over the weak link. Wider bridges can show a significant current-phase relationship as well, provided the width of the bridge is comparable to, or smaller than, the effective London penetration depth $\lambda_\perp$. The most used values for the bulk penetration depth for MgB_2 vary from 140 to 180 nm [10], yielding an effective penetration depth, $\lambda_\perp = \lambda_L \coth(d/2\lambda_L)$ of 230 to 360 nm for films with a thickness d of 200 nm. This current- phase relationship was exploited to fabricate the first MgB_2 SQUIDs [11].

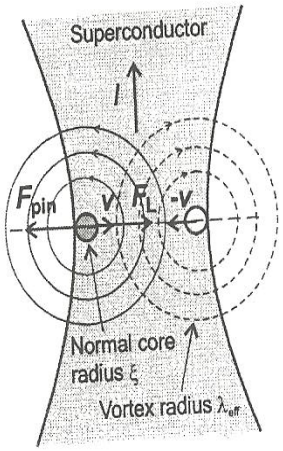

Fig. 5: Schematic drawing of the forces acting on two Abrikosov vortices in a nanobridge .

3.3. Electrical Characteristics

The electrical characteristics of the nanobridges were measured in a four point configuration in a shielded cryostat, like the properties of Josephson junctions described in section 2.2. The films with nano bridges showed unchanged values of T_C (~ 40 K) as compared to the films before structuring. The typical current- voltage characteristics above 10 K resemble the I-V characteristics presented in Fig.7 (a). In this Figure the non-hysteretic current voltage

characteristics of a 140 nm wide nanobridge at 22 K is shown. Below 10 K a small hysteresis appears in some cases, which can differ from bridge to bridge. The nanobridges showed a very high critical current density of $5x10^7$A/ cm^2 at 4.2 K. This value of critical current density is comparable to the highest one reported in bulk material.

To investigate how critical current density changes with small variations in the nanobridges width, we compared J_C of 100 nm and 140 nm wide nanobridges. The dependence of the critical current vs. temperature for two different nanobridges is illustrated in Fig.7 (b). Using SRIM (Stopping and Range of Ions in Matter) software, version SRIM- 2000.40, which can calculate the penetration depth of ions in MgB_2 films, we obtained the value of about 20 nm. This is consistent with the data presented in Fig.7 (b) and can explain a small difference in J_c value for both nanobridges in a way that the effective area, through which the current is passing, is smaller than the one estimated from FIB profile due to the damages caused by Ga ions. However, from the considerable spread in the J_c data for other nanobridges of the same widths one may rule out that the fit of this 20 nm Ga ion damages into the effective area could be coincidental. The depairing current density can be estimated for the single band case by $J_0 = 4B_C/ [3\sqrt{6}\mu_0 \lambda]$, where B_C is a thermodynamic critical field defined as $B_C = \Phi_0 / 2\sqrt{2}\pi\lambda\xi$,
$\Phi_0 = h/2e$ is the flux quantum, λ is the penetration depth and ξ is the coherence length [12]. For MgB_2, by taking λ_{ab} (0) ~ 62 nm and ξ_{ab} (0) ~ 5 nm [18], J_0 can be estimated to be ~ $2x10^9$A/ cm^2. The highest J_C's of the HPCVD films are in the order of 10^7A/cm^2 (as shown in Fig.7 (b)). The J_C value in nano bridges is limited by the flux flow motion and not by the depairing mechanism, which explains the lower J_C value than the depairing current density.

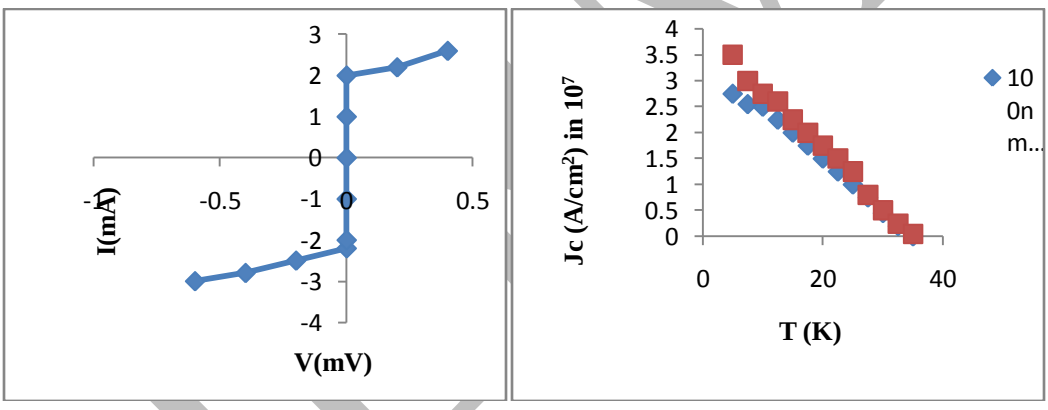

(a) (b)

Fig. 7 (a) Current-voltage characteristics of a 140 nm wide nano bridge at T = 22 K; (b) Critical current vs. temperature for nano bridges of 100 nm and 140 nm width.

4. CONCLUSIONS AND OUTLOOK

The fabrication of MgB_2 weak links in the form of Josephson junctions and nano bridges presents an important step for further implementation of MgB_2 into electronics and superconducting sensors. Our work on ramp-type Josephson junctions based on PLD films resulted in the modulation of the junction's critical current in applied magnetic field and the appearance of Shapiro steps by applied microwave irradiation. The potential of achieving RSJ- behavior and relatively high operating temperatures make MgB_2 ramp- type junctions very suitable for electronic circuits. To achieve the potentially large I_CR_N - product in MgB_2 tunnel junctions, which is of interest for electronic application, the quality of thin films with respect to smoothness, film epitaxy as well as an artificial barrier- layer quality has to be improved.

Considerable improvements of the junction properties can be expected by using smooth, epitaxially grown thin films with bulk- like critical temperature values for the fabrication of the Josephson junctions. Suitable films would be the films prepared by the HPCVD since they fulfill the above- mentioned requirements. It is expected that a low surface roughness (about 2 nm) would result in the absence of shunting channels (pinholes) that would considerably improve the properties of the junctions.

REFERENCES:

1. D. C. Larbalastier et al., Nature 410, 186(2001).
2. A. Brinkman et al., Phys. Rev. B 65, 180517(R) (2002).
3. J. Gao,W.A. M. Aarnink, G. J. Gerritsma, and H. Rogalla, Physica C 171, 126(1990).
4. D. Mijatovic et al., Appl. Phys. Lett. 80, 2141(2002).
5. B. H. Moeckly and K. Char, Appl. Phys. Lett. 71, 2526 (1997).
6. M. Faucher et al., Physica C 368, 211(2002).
7. S. K. Lam and D. L. Tilbrook, Appl. Phys. Lett. 82, 1078(2003).
8. M. V. Pedyash, D. H. A. Blank, J. H. de Muijnck, H. Rogalla, IEEE Trans. Appl. Supercond. 7, 2764(1997).
9. M. R. Eskildsen et al., Phys. Rev. Lett. 89, 187003(2002).
10. D. K. Finnemore, J. E. Ostenson, S. L. Bud'ko, G. Lapertot, P. C. Canfield, Phys. Rev. Lett. 86, 2420(2001).
11. S. Y. Xu et al., Phys. Rev. B 68, 224501(2003).
12. T.G. Lee at al., Physica C: Superconductivity, 15-20, 468, (2008).
13. J. Yang at al., Physica C: Superconductivity, 1-2, 467, (2007).
14. K. Nishiyuki, Physica C: Superconductivity, 21-22, 471, (2011).
15. K. Yamazaki and M. Naito, Physica C, 495 (2013).
16. E. Altin at al., Current Applied Physics, 3, 14 (2014).